Magnetism of a FeO(111)/Fe(110) surface

K. Mori, M. Yamazaki, T. Hiraki, H. Matsuyama, and K. Koike
Department of Physics, Hokkaido University, Sapporo 060-0810, Japan
(Received 12 August 2004; revised manuscript received 28 March 2005; published 8 July 2005)

By comparing the oxidation dependencies of the polarizations of secondary electrons emitted from FeO(111)/Fe(110) and FeO(001)/Fe(001), we confirmed that the FeO(111) surface is ferromagnetically ordered even above a bulk Néel temperature of 198 K, and the magnetic surface layer is antiferromagnetically coupled with the underlying ferromagnetic Fe(110) substrate through paramagnetic FeO. A possible cause of the ferromagnetic order at the FeO(111) surface is reconstruction and we propose a concrete model that can explain the ferromagnetic order.

DOI: 10.1103/PhysRevB.72.014418 PACS number(s): 75.70.Rf, 75.70.Ak, 79.20.Hx

The surfaces of solids generally show different properties from those of bulk regions because the translational symmetry is broken. Magnetism is no exception. Liebermann *et al.* reported that there is a magnetically dead layer at the surface of ferromagnetic Fe[1] and Ni.[2] This sensational claim, however, was denied by the works of Shinjo *et al.*[3,4] and Gradmann.[5] A decade later, opposite systems, i.e., ferromagnetic order at the surfaces of paramagnetic 3*d* metals were reported. Klebanoff *et al.*,[6] by using photoemission spectroscopy, found ferromagnetic order at the Cr surface at above the bulk Néel temperature. Rau *et al.*, by using electron capture spectroscopy, also found such order at the V surface[7] and at the Gd surface[8] at above bulk Curie temperature. In a previous paper, we showed evidence that the surface of a 3*d* metal oxide, FeO(111) formed on Fe(110), was ferromagnetically ordered even above the bulk Néel temperature of 198 K, and suggested that this order was probably caused by surface reconstruction.[9] Kim *et al.* conducted a similar experiment and obtained the same result as ours.[10] However, they proposed a different interpretation claiming that the oxide is ferrimagnetic Fe_3O_4 and that our interpretation of the ferromagnetic order at the FeO(111) surface is wrong. In this paper, we present additional experimental data and considerations that support our previous interpretation. We also propose a concrete surface-reconstructed model that can explain the surface ferromagnetic order.

The apparatus used in the experiment is described elsewhere.[11] The sample chamber was equipped with a heating, cooling, temperature-monitoring, and magnetic-field-applying sample stage; an electron gun of 0.05–5 keV; and a $\leqslant$1-mm ϕ probe beam for secondary electron excitation, a scanning-type ion gun that produced a 0.5–5-keV, $\geqslant$0.5-mm ϕ Ar^+-ion beam. It also had a cylindrical mirror analyzer and a Mott detector for the energy and polarization analyses of secondary electrons. Besides this it had a low-energy electron diffraction (LEED) system for crystallinity analysis, an Auger electron spectroscope (AES) for element analysis, and an oxygen gas inlet system. The sizes of the Fe(110) and Fe(001) samples were both $16\times6\times1$ mm^3 with the [001] and [010] axes in the length direction, respectively. The natural domain width of the samples was approximately a few hundred microns according to Kerr microscope observations, and this width may be smaller than the probe-electron-beam diameter. Thus the sample was mounted on a horseshoe-shaped electromagnet so that it had a single-domain structure, with its magnetization in the [001] or $[00\bar{1}]$ directions for Fe(110) and the [010] or $[0\bar{1}0]$ directions for Fe(001) in a remnant state after the application of a magnetic field. The secondaries were obtained from the uniform magnetization area. The vacuum pressure inside the sample chamber was in the middle of the 10^{-10} Torr range. The Fe samples were cleaned by 2–5-keV Ar^+-ion bombardment followed by flash heating to 860 K. These samples were kept at the temperature described below and exposed to an oxygen atmosphere of 1.0×10^{-6} Torr to form an oxide layer. The surface cleanliness of Fe samples and the stoichiometry of the oxides were studied by AES, all with a 3-keV primary, and the surface crystal structures of these samples were studied by LEED.

The surface magnetism was studied with the apparatus as follows. After exposure, oxygen was evacuated and the sample was cooled down to 370 K by attaching the sample holder to a liquid nitrogen reservoir. We started polarization measurement as soon as the sample temperature was $\sim$370 K, by detaching the sample from the reservoir. The sample was then irradiated with a 2-keV electron beam and the emitted secondary electrons were directed through the energy analyzer to a Mott detector to measure polarization as a function of secondary energy. The resolution of the energy analyzer was $\sim$0.7 eV. To cancel out offset polarization, which was a few percent, arising from apparatus asymmetry, we detected respective polarizations P_+ and P_- for magnetization in the [001] and $[00\bar{1}]$ directions for Fe(110) and in the [010] and $[0\bar{1}0]$ directions for Fe(001), and we obtained final polarization $P=(P_++P_-)/2$. When the experiment ended, the sample temperature was $\sim$350 K.

Figure 1 shows the AES spectra at a 3-keV primary and the LEED patterns (a) for clean Fe(110) and (b) for Fe(110) exposed to 3600 L of O_2 at 570 K. The LEED pattern is obtained with a primary at 93 eV for (a) and 60 eV for (b). The LEED for the clean Fe(110) shows a typical bcc (110) surface pattern. From the sixfold symmetric LEED pattern with $p(2\times2)$ satellites in (b), we can see that the oxide surface is reconstructed (111). The composition of thin oxide films on iron has been reported to be FeO, Fe_2O_3, or Fe_3O_4, depending on the surface index of the substrate, the preparation temperature, and the analysis technique.[12] It has been

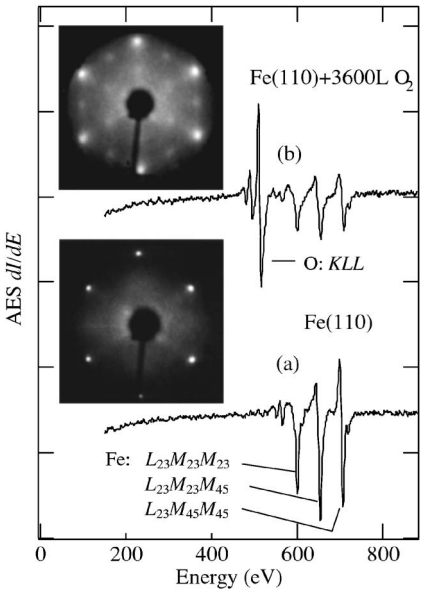

FIG. 1. AES spectra at 3-keV primary, where Auger transition is labeled for each peak, and the LEED patterns (a) for clean Fe(110) and (b) for Fe(110) exposed to 3600 L of O_2 at 570 K. The LEED pattern is obtained by a primary at 93 eV for (a) and 60 eV for (b).

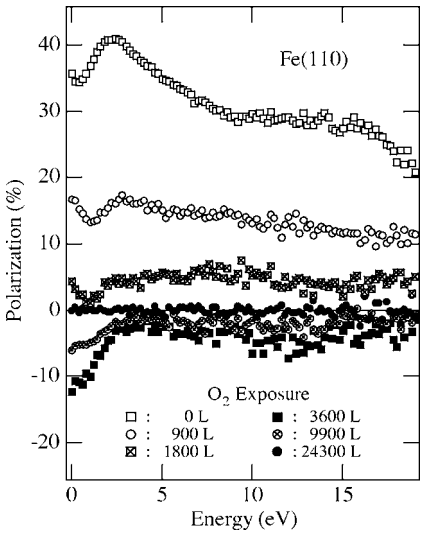

FIG. 2. Secondary polarizations for FeO/Fe(110) as a function of secondary energy for the selected oxygen exposures from 0 L to 24 300 L.

reported, however, that the oxide layer formed when Fe(110) is exposed to oxygen at a temperature higher than 470 K is FeO(111).[13,14] Thus, the oxide films obtained in this work were expected to be FeO(111). We confirmed this by quantitative Auger analysis. Because the Auger sensitivity of O(*KLL*) relative to Fe($L_{23}M_{23}M_{45}$) is 2.6,[15] the AES peak ratios of O(*KLL*)/Fe($L_{23}M_{23}M_{45}$) for FeO, Fe_3O_4, and Fe_2O_3 should be 2.6, 3.5, and 3.9. The ratio obtained from Fig. 1(b) is 2.9±0.1, which favors FeO over Fe_3O_4 or Fe_2O_3. This value is comparable to the 3.0–3.2 observed for FeO by Kelemen *et al.*;[16] however, it is much smaller than the 4.5±0.4 observed for Fe_3O_4 by Ertl and Wandelt.[17]

Another way to confirm the formation of FeO is by analyzing the ratios of the three Fe Auger peaks, $L_{23}M_{23}M_{23}$, $L_{23}M_{23}M_{45}$, and $L_{23}M_{45}M_{45}$. According to Rao *et al.*,[18] the peak ratios, $L_{23}M_{45}M_{45}/L_{23}M_{23}M_{45}$, $L_{23}M_{45}M_{45}/L_{23}M_{23}M_{23}$, and $L_{23}M_{23}M_{45}/L_{23}M_{23}M_{23}$ are 0.85, 1.22, and 1.42 for FeO; 0.79, 0.96, and 1.22 for Fe_3O_4; and 0.77, 0.93, and 1.21 for Fe_2O_3, respectively. The differences in the ratios among the oxides, however, are smaller than in O(*KLL*)/Fe($L_{23}M_{23}M_{45}$), and there may be AES system dependency. Therefore, we first compared the three ratios among Fe peaks obtained from the spectrum in Fig. 1(a) with the ratios of 1.13, 1.70, and 1.50 obtained by Rao *et al.*[18] Our respective ratios were 1.06±0.02, 1.61±0.03, and 1.52±0.03, which had good agreement with Rao *et al.* This warranted quantitative investigation using our AES system. The respective Auger peak ratios among Fe peaks obtained from the spectrum for oxidized Fe(110) in Fig. 1(b) were 0.91±0.03, 1.25±0.05, and 1.38±0.06, which agreed well with those for FeO reported by Rao *et al.* but which clearly differed from the values they reported for Fe_3O_4 and Fe_2O_3. Based on the above considerations, we concluded that the oxide formed on the Fe(110) surface was FeO(111).

Figure 2 shows secondary polarizations as a function of secondary energy for selected oxygen exposures from 0 L to 24 300 L. Figure 3 shows secondary polarizations as a function of oxygen exposure for secondary energies of 0 eV and 10 eV together with an Auger peak ratio of O(*KLL*)/Fe($L_{23}M_{23}M_{45}$). The polarization spectrum for clean Fe(110) in Fig. 2 shows the same behavior as that observed by Kirschner and Koike,[19] where the spectrum was characterized by a peak at 2 eV and a shoulder at around 17 eV. The polarizations decreased with oxygen exposure, and surprisingly, they changed polarity between exposures of 1800 L and 2700 L (see Fig. 3) for all observed energies between 0 and 19 eV. At the 3600 L exposure, polarization as a whole reached a negative maximum, and it became zero at 24 300 L. This exposure dependency of polarization can more clearly be seen in Fig. 3. In the figure, the Auger peak ratio of O(*KLL*)/Fe($L_{23}M_{23}M_{45}$) increases with oxygen exposure up to 3600 L and remains constant at 2.9±0.1 after that. This means that the oxide is FeO, at least for oxygen

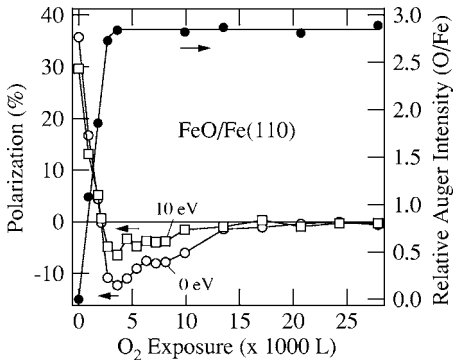

FIG. 3. Secondary polarizations and Auger peak ratios of O(*KLL*)/Fe($L_{23}M_{23}M_{45}$) for FeO/Fe(110) as a function of oxygen exposure. The polarizations are for secondary energies of 0 eV and 10 eV. The solid line for Auger peak ratios is just a guide for the eyes.

exposure of more than 3600 L. A hexagonal LEED pattern [Fig. 1(b)] appears at 900 L and remains the same after that.

Because secondary polarization reflects magnetization of the sample surface,[20] the observations in Figs. 2 and 3, where the polarization for FeO(111) has an opposite polarity to that for underlying Fe(110), indicate that the surface of FeO(111) is ferromagnetically ordered with magnetization antiparallel to that of the Fe(110). The antiparallel arrangement of magnetization of the FeO(111) surface and that of the underlying Fe(110) may be caused by Ruderman-Kittel-Kasuya-Yosida (RKKY)-like interaction[9] as observed for nonmagnetic or magnetic multilayered film that has giant magnetoresistance.[21] A different interpretation was given for this behavior by Kim *et al.*[10] They studied the magnetism of Fe(110) thin film exposed at 570 K to O_2 until 1500 L. They reported that the produced oxide was Fe_3O_4 and its magnetization was antiparallel to that of the Fe(110) due to the direct exchange interaction. The difference in the oxides obtained by them and us is probably due to the different experimental systems and procedures. We obtained iron oxide by exposing a bulk Fe(110) at 570 K to 1×10^{-6}-Torr O_2 with the total exposure of more than 2000 L. On the other hand, they obtained iron oxide by exposing a 100 monolayer (ML) thick film Fe(110) at 523 K to 5×10^{-7}-Torr O_2 with a total exposure of less than 1500 L. The oxide obtained by Kim *et al.* may be Fe_3O_4. We are confident, however, that our oxides are unambiguously FeO from the quantitative AES analysis as described above. Because the obtained oxides are different, direct comparison of the magnetism of the two oxides obtained by us and by Kim *et al.* is not appropriate

As shown in a previous paper,[9] the ferromagnetic layers are localized at the surface region to a depth of a few monolayers, and the FeO thickness is estimated to be about 50 Å for 3600 L of oxygen exposure, when the polarization reaches a negative maximum. The zero polarization observed in Figs. 2 and 3 for the thicker FeO layer, obtained by more than 24 300 L of oxygen exposure, can be explained by a RKKY-like interaction. Because the RKKY-like interaction decreases with increasing distance, there is no interlayer coupling between the magnetization of the Fe(110) substrate and that of the surface of the thicker FeO(111). When there is no interlayer coupling, magnetization at the FeO(111) surface might have a distribution different from that of the underlying Fe(110) substrate, e.g., a multidomain structure producing zero average polarization. Another possibility is that the surface ferromagnetic order is stabilized by RKKY-like interaction. In this case, the surface ferromagnetic order becomes less stable with the increase in FeO layer thickness and finally disappears.

To examine whether the surface ferromagnetic order is inherent in FeO(111), we formed FeO(001) by oxidizing Fe(001) and studied its magnetism. The preparation method of the sample was the same as that for Fe(110) except for the oxidization temperature. The composition of oxide on Fe(001) is still controversial. Leibbrandt *et al.* reported that the oxide formed by exposing Fe(001) at 573 K to 7.5×10^{-7} -Torr O_2 is FeO.[22] On the other hand, Flis-Kabulska *et al.* reported that the oxide formed by exposing Fe(001) at 550 K to 7.5×10^{-7}-Torr O_2 is Fe_3O_4.[23] We first formed the oxide by exposing the Fe(001) at 570 K to 1×10^{-6}-Torr O_2, which are the same conditions as when we formed the FeO on Fe(110). Both the AES spectrum and LEED pattern show that the oxide is Fe_2O_3 or Fe_3O_4, where the latter supports the results of Flis-Kabulska *et al.* There is a consensus that FeO tends to be formed at higher temperatures[24] because Fe ions move more easily to the surface from the substrate through the oxide layer. Thus, in this experiment, we formed an oxide by exposing Fe(001) at 773 K, which was 200 K higher than that for Fe(110), to 1×10^{-6}-Torr O_2.

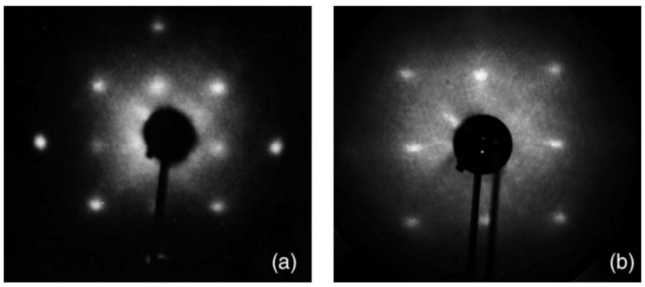

FIG. 4. LEED patterns (a) for clean Fe(001) and (b) for Fe(001) exposed to 7200 L of O_2 at 773 K, which is obtained by a primary at 187 eV for (a) and 154 eV for (b).

Figure 4 shows the LEED patterns (a) for clean Fe(001) and (b) for Fe(001) exposed to 7200 L of O_2 at 773 K. The LEED pattern is obtained primarily at 187 eV for (a) and 154 eV for (b). The LEED pattern for the clean Fe(001) shows a typical bcc (001) surface pattern. If we assume the LEED pattern (b) is for the fcc (001) surface where the [100] axis rotates by 45° from the [100] axis of Fe(001), the lattice constant of the fcc structure is analyzed to be 4.4±0.1 Å. This value is in good agreement with that of FeO's 4.29Å. Because the lattice constant of Fe is 2.86Å, the 45° -rotated FeO(001) growth on the Fe(001) is plausible, because the lattice mismatch between the two is 6%.

Figure 5 shows polarizations of secondary electrons emitted from the oxide as a function of secondary energy for selected oxygen exposures from 0 L to 19 800 L. Figure 6 shows secondary polarizations as a function of oxygen exposure for secondary energies of 0 eV and 10 eV together with the Auger peak ratio of O(*KLL*)/Fe($L_{23}M_{23}M_{45}$). In Fig. 6, polarization is plotted on a logarithmic scale, without the values at the exposure of 27 000 L and 37 800 L, because these values are comparable to the noise level. Thus we can analyze the surface magnetism conveniently, as described later. The polarization spectrum for clean Fe(001) in Fig. 5 shows behavior similar to that observed by Allenspach *et al.*[25] where the spectrum was characterized by a bump at around 10 eV. The magnitude of the polarization, however, is smaller as a whole than that of Allenspach *et al.* and of the clean Fe(110) shown in Fig. 2. We think that one reason for the discrepancy is probably the pinned magnetic domains in the Fe(001), which were not inverted by the applied magnetic field. Different from the case of Fe(110), the polarizations decreased monotonically with oxygen exposure for all observed energies between 0 and 20 eV without any change of the polarization sign and became almost zero at 19 800 L. This exposure dependency of polarization can be more

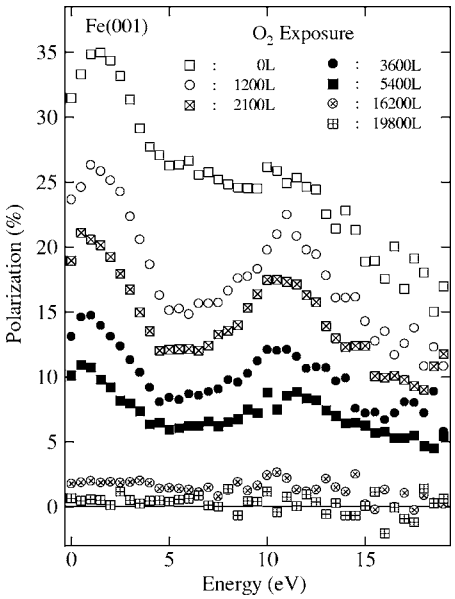

FIG. 5. Secondary polarizations for FeO/Fe(001) as a function of secondary energies for the selected oxygen exposures from 0 L to 19 800 L.

clearly seen in Fig. 6. This result shows a strong contrast to the case of the Fe(110). In the figure, the Auger peak ratio of O(*KLL*)/Fe($L_{23}M_{23}M_{45}$) increases with oxygen exposure up to 5400 L and remains constant at 2.7±0.1 after that. This value is a little smaller than the 2.9±0.1 for the case of FeO(111)/Fe(110). The LEED pattern shown in Fig. 4(b) remained unchanged until the maximum exposure in the experiment. Considering these results, the oxide grown on Fe(001) is FeO(001), at least for the thickness range for oxygen exposure of more than 5400 L.

From the results in Figs. 5 and 6, we can exclude the ferromagnetic order at the FeO(001) surface with the magnetization antiparallel to that of underlying Fe(001), because negative polarization is never observed, different from the case of FeO(111). The possibility of the ferromagnetic order with the magnetization parallel to that of underlying Fe(001)

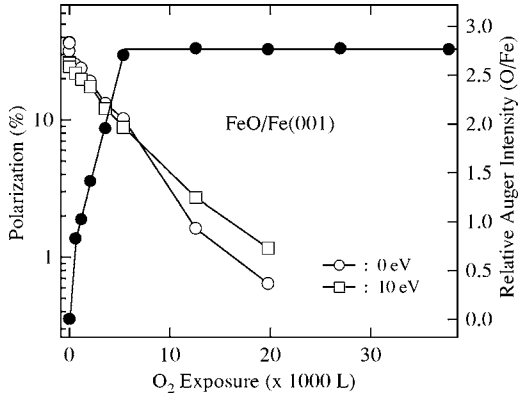

FIG. 6. The secondary polarizations and Auger peak ratios of O(*KLL*)/Fe($L_{23}M_{23}M_{45}$) for FeO/Fe(001) as a function of oxygen exposure. The polarizations are for the secondary energies of 0 eV and 10 eV. The solid line for Auger peak ratios is just a guide for the eyes.

is also excluded as follows. When a ferromagnet is covered by a paramagnetic thin film, the secondary polarization decreases almost exponentially with the film thickness, and if there is a thickness-dependent ferromagnetic order, fine structures are superimposed on the polarization decay curve.[26] The experimental results in Fig. 6 show that the polarization decreases almost exponentially without any fine structures. This fact strongly suggests that the reduction of secondary electron polarization as oxidation proceeds is due to a growing paramagnetic FeO layer, and there is no ferromagnetic order at the surface. The 0 eV secondary polarization initially decreases faster than 10 eV one. This is thought to be due to the reduced polarization-enhancement effect,[27,28] which is characteristic of a 3*d* magnet having an asymmetric density of state with respect to spin. This disappearance of the enhancement effect also suggests that oxides formed at the surface are nonmagnetic, which is consistent with the oxide being FeO. Before the secondary electron polarization becomes zero, the Auger peak ratio reaches a constant value of 2.7±0.1, which almost agrees with the value of 2.6 expected for FeO. Regarding the oxidation process, Leibbrandt *et al.* showed that the speed of oxidation is much faster for Fe(001) than Fe(110).[29] Comparing the Auger peak ratios in Figs. 3 and 6, however, we can see that the oxidation speed of Fe(001) at 773 K is rather slower than that of Fe(110) at 573 K. Because the higher the oxidation temperature, the faster the oxidation, our results seem to contradict the results of Leibbrandt *et al.* The contradiction is probably due to faster sublimation of the iron-oxide molecules on Fe(001) than on Fe(110), because the oxidation temperature was higher for Fe(001) than for Fe(110). As a result, the oxidation speed seems to decrease for Fe(001).

From the experimental results mentioned above, we can see that the observed surface magnetism is inherent in FeO(111) but not in FeO(001). This fact excludes the possibility that the surface magnetism observed for FeO(111) is due to bulklike magnetic Fe_3O_4 or γ-Fe_2O_3. This is because, if Fe_3O_4 or γ-Fe_2O_3were the origin of the ferromagnetism, we should also observe ferromagnetism at the FeO(001) surface. However, this is not the case.

We next consider the origin of the ferromagnetic order at the surface of the FeO(111). The FeO has a NaCl structure. The (111) surface of such a structure is polar, where the positively and negatively charged layers are alternatively stacked in the [111] direction. This configuration causes a macroscopic electric field in the bulk region and the structure is energetically unstable. This instability can be removed if the surface is reconstructed with an appropriate charge distribution.[30] One such reconstruction, called octopolar reconstruction, is reported for NiO,[31,32] which has the same NaCl structure as FeO. In this structure, three of the four $O^{2-}(Fe^{2+})$ ions in the top layer and one of the four $Fe^{2+}(O^{2-})$ ions in the second layer are removed. This reconstruction at the surface causes no macroscopic electric field in the bulk region. The $p(2\times2)$ LEED patterns observed both in Fig. 1 and by Cappus *et al.*[14] for FeO(111) are not inconsistent with octopolar reconstruction. For this structure, however, we cannot expect a surface ferromagnetic order.[9] Concerning the (111) surface of the NaCl structure, not only octopolar reconstruction but also another type has been reported. Barbier *et*

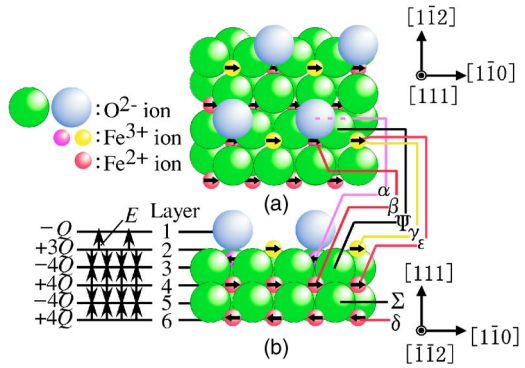

FIG. 7. (Color online) Lattice structure of FeO(111) with a reconstruction, where (a) is the top view and (b) is the side view of the (001) cross section observed along [1$\bar{1}$2] direction. Here, some Fe^{2+}, Fe^{3+}, and O^{2-} ions are labeled by Greek characters. Three of the four O^{2-} ions in the top layer and two of the four Fe^{2+} ions in the second layer are absent. The remaining iron ions in the second layer are Fe^{3+} and are at two different sites: one, labeled by α (pink), just under the O^{2-} ions (light blue) in the top layer, i.e., the tetrahedral position among the O^{2-} ions, and the other, labeled by γ (yellow), at above the center of the triangle made by the O^{2-} ions (green) in the third layer. These iron ions are colored differently from the bulk ones (red). There are two different sites of Fe^{2+} ion positions in the fourth layer, as labeled by β and ε (both are red). The arrows inside the Fe^{2+} or Fe^{3+} ions indicate magnetic moments if the sample is below the Néel temperature. The left side of (b) shows the layer number counted from the top, and layer dependence of the electric charge, where the values $-Q$, $+3Q$, $\pm 4Q$ at the extreme left are charge density per unit area of the layer, and electric field $\boldsymbol{E}$. This structure does not cause any macroscopic electric field in the bulk region, and ferromagnetic order at the surface is expected.

al. studied the NiO(111) surface obtained by annealing a bulk Ni(111) sample in 10^{-4}-mbar O_2 above 700 K.[33] They suggested that Ni_3O_4(111) spinel-like reconstruction occurred at the NiO(111) surface by analyzing the x-ray diffraction pattern.

Although it is obvious from the LEED pattern that the FeO(111) surface reconstructs, the actual structure has not yet been identified. In Fig. 7, we suggest a new surface-reconstructed structure, which can be expected to induce ferromagnetic order. Figure 7(a) is a top view and Fig. 7(b) is a side view of the FeO(111) surface region. In this structure, three of the four O^{2-} ions in the top layer and the two of the four Fe^{2+} ions in the second layer are absent. The remaining iron ions in the second layer are Fe^{3+} and are at two different sites: one, labeled by α (pink), just under the O^{2-} ions in the top layer, i.e., the tetrahedral position among the O^{2-} ions, and the other, labeled by γ (yellow), at above the center of the triangle made by the O^{2-} ions in the third layer. These iron ions are colored differently from the bulk ones (red). There are two different sites of Fe^{2+} ion positions in the fourth layer, as labeled by β and ε (both are red). The left side of Fig. 7(b) shows the layer number counted from the top and layer dependence of the electric charge, where the values at extreme left are the charge density per unit area of the layer. $\boldsymbol{E}$ indicates electric field. As can be seen from the $\boldsymbol{E}$ distribution, this configuration causes no macroscopic electric field in the bulk. Moreover, the expected LEED pattern is $p(2\times 2)$ as observed by the experiment.

We considered the possibility of ferromagnetic order in this surface structure. In this reconstruction, the angles φ made by Fe-O-Fe ions are $0.39\pi(\angle\gamma\Psi\varepsilon)$, $0.41\pi(\angle\alpha\Psi\beta)$, $0.50\pi(\angle\beta\Psi\varepsilon)$, $0.73\pi(\angle\beta\Psi\gamma)$, $0.91\pi(\angle\alpha\Psi\varepsilon)$, and $\pi(\angle\beta\Sigma\delta)$. The magnitude and sign of the superexchange energy J depend on the angle φ and J is negative for $\varphi=\pi$ and J is positive for $\varphi=\pi/2$.[34] We approximated $J=J_+$ (positive) for $\varphi=0.39\pi$, 0.41π, and 0.50π, $J=0$ for $\varphi=0.73\pi$, and $J=J_-$ (negative) for $\varphi=0.91\pi$ and π. We calculated the superexchange energy, J_S, per Fe^{2+} ion in the fourth layer to be $3.75J_-+5.25J_+$. On the other hand, the superexchange energy, J_B, per Fe^{2+} ion in the bulk layer is calculated to be $6J_-$. We do not know the real values of J_+ and J_-, but if $J_+ < 1.7J_-$ is satisfied, we can expect surface ferromagnetic order even above the bulk Néel temperature of 198 K. Moreover, this reconstruction can explain the AES peak ratio $O(KLL)/Fe(L_{23}M_{23}M_{45})$ of around 2.9 ± 0.1 observed for the as-prepared FeO(111) in Figs. 1 and 3, and 2.7 ± 0.1 observed for Fe(001) in Fig. 6, and also 2.6 observed for sputtered FeO(111) in Ref. 9. As can be seen from Fig. 7(a), more O^{2-} ions are visible at the surface than Fe^{2+} or Fe^{3+} ions. This probably makes the AES peak ratio $O(KLL)/Fe(L_{23}M_{23}M_{45})$ for this reconstructed FeO(111) slightly larger than that for the FeO(001) and sputtered one, where the ratio of iron and oxygen ions is probably 1:1, giving an AES peak ratio of around 2.6. If we apply the scenario described above to the FeO(001), surface magnetism cannot be expected. Each (001) layer of the NaCl-structure FeO has the same amount of cations and anions with the same magnitude of electric charges, and the net charge is zero in the layer. Thus the surface is not polar and the structure is electrostatically stable without surface reconstruction, which is the origin of the surface magnetism of FeO(111). In fact, our experiment does not show surface ferromagnetism at FeO(001), supporting the above considerations.

In summary, we studied the surface magnetism of FeO(111)/Fe(110) and FeO(001)/Fe(001) at around 360 K by using spin-polarized secondary electrons. In the case of FeO(111)/Fe(110), as the oxidation progresses, the polarization decreases and changes from positive to negative, finally becoming zero for thick FeO(111). In the case of FeO(001)/Fe(001), however, secondary polarization decreases monotonically to zero. Comparing these two experimental results, we confirmed that the FeO(111) surface is ferromagnetically ordered even above a bulk Néel temperature of 198 K, and the surface ferromagnetic layer is antiferromagnetically coupled to the Fe(110) substrate by RKKY-like interaction through paramagnetic FeO. A possible cause of the ferromagnetic order at the FeO(111) surface is reconstruction, and we proposed a concrete model that can explain the ferromagnetic order. In the model, the polar FeO(111) surface is reconstructed to decrease the electrostatic energy of the FeO(111) surface, and the new configuration of iron and oxygen ions induces the surface ferromagnetic order.

The missing ferromagnetic order at the FeO(001)/Fe(001) surface, at which the reconstruction does not occur because its surface is electrostatically stable, supports the validity of the proposed model.

We thank Professor H.-J. Freund of the Ruhr-Universität Bochum, Dr. S. Watanabe of the University of Tokyo, Dr. A. Sakuma of Hitachi Metals, Ltd., and Dr. M. Ichimura of ARL, Hitachi, Ltd. for their valuable discussions.

[1] L. Liebermann, D. R. Fredkin, and H. B. Shore, Phys. Rev. Lett. **22**, 539 (1969).
[2] L. Liebermann, J. Clenton, D. M. Edwards, and J. Mathon, Phys. Rev. Lett. **25**, 232 (1970).
[3] T. Shinjo, T. Matsuzawa, T. Takada, S. Nasu, and Y. Murakami, Phys. Lett. **36A**, 489 (1971).
[4] T. Shinjo, T. Matsuzawa, T. Takada, S. Nasu, and Y. Murakami, J. Phys. Soc. Jpn. **35**, 1032 (1973).
[5] U. Gradmann, Appl. Phys. **3**, 161 (1974).
[6] L. E. Klebanoff, S. W. Robey, G. Liu, and D. A. Shirley, Phys. Rev. B **30**, 1048 (1984).
[7] C. Rau, C. Liu, A. Schmalzbauer, and G. King, Phys. Rev. Lett. **57**, 2311 (1986).
[8] C. Rau and S. Eichner, Phys. Rev. B **34**, 6347 (1986).
[9] K. Koike and T. Furukawa, Phys. Rev. Lett. **77**, 3921 (1996).
[10] H.-J. Kim, J.-H. Park, and E. Vescovo, Phys. Rev. B **61**, 15284 (2000).
[11] K. Koike, T. Furukawa, G. P. Cameron, and Y. Murayama, Phys. Rev. B **50**, 4816 (1994).
[12] G. W. R. Leibbrandt, S. Deckers, M. Wiegel, and F. H. P. M. Habraken, Surf. Sci. **244**, L101 (1991).
[13] G. W. R. Leibbrandt, L. H. Spiekman, and F. H. P. M. Habraken, Surf. Sci. **287/288**, 250 (1993).
[14] D. Cappus, M. Haßel, E. Neuhaus, M. Heber, F. Rohr, and H.-J. Freund, Surf. Sci. **337**, 268 (1995).
[15] L. E. Davis, N. C. MacDonald, P. W. Palmberg, G. E. Riach, and R. E. Weber, *Hand Book of Auger Electron Spectroscopy*, 2nd ed. (Physical Electronics Industries, Inc., Edina, Minnesota, 1978).
[16] S. R. Kelemen, A. Kaldor, and D. J. Dwyer, Surf. Sci. **121**, 45 (1982).
[17] G. Ertl and K. Wandelt, Surf. Sci. **50**, 479 (1975).
[18] C. N. R. Rao, D. D. Sarma, and M. Hegde, Proc. R. Soc. London, Ser. A **370**, 269 (1980).
[19] J. Kirschner and K. Koike, Surf. Sci. **273**, 147 (1992).
[20] G. Chrobok and M. Hofmann, Phys. Lett. **57A**, 257 (1976).
[21] P. Bruno and C. Chappert, Phys. Rev. Lett. **67**, 1602 (1991).
[22] G. W. R. Leibbrandt, G. Hoogers, and F. H. P. M. Habraken, Phys. Rev. Lett. **68**, 1947 (1992).
[23] I. Flis-Kabulska, B. Handke, N. Spiridis, J. Haben, and J. Korecki, Surf. Sci. **507**, 865 (2002).
[24] S. J. Roosendaal, B. van Asselen, J. W. Elsenaar, A. M. Vredenberg, and F. H. P. M. Habraken, Surf. Sci. **442**, 329 (1999).
[25] R. Allenspach, M. Taborelli, and M. Landolt, Phys. Rev. Lett. **55**, 2599 (1985).
[26] T. Furukawa and K. Koike, Surf. Sci. **347**, 193 (1996).
[27] H. Hopster, R. Raue, E. Kisker, G. Guntherodt, and M. Campagna, Phys. Rev. Lett. **50**, 70 (1983).
[28] D. R. Penn, S. P. Apell, and S. M. Girvin, Phys. Rev. Lett. **55**, 518 (1985).
[29] G. W. R. Leibbrandt, L. H. Spiekman, and F. H. P. M. Habraken, Surf. Sci. **287/288**, 245 (1993).
[30] D. Wolf, Phys. Rev. Lett. **68**, 3315 (1992).
[31] F. Rohr, K. Wirth, J. Libuda, D. Cappus, M. Bäumer, and H.-J. Freund, Surf. Sci. **315**, L977 (1994).
[32] C. A. Ventrice, Jr., T. Bertrams, H. Hannemann, A. Brodde, and H. Neddermeyer, Phys. Rev. B **49**, 5773 (1994).
[33] A. Barbier, C. Mocuta, and G. Renaud, Phys. Rev. B **62**, 16056 (2000).
[34] J. Kanamori, J. Phys. Chem. Solids **10**, 87 (1959).